



# Magnetic structuring at spatially unresolved scales

J. O. Stenflo

Institute of Astronomy, ETH Zurich, HIT J 23.6, CH-8093 Zurich, and  
Istituto Ricerche Solari Locarno (IRSOL), Via Patocchi, CH-6605 Locarno-Monti  
e-mail: [stenflo@astro.phys.ethz.ch](mailto:stenflo@astro.phys.ethz.ch)

**Abstract.** Magneto-convection structures the Sun's magnetic field down to the magnetic diffusion scale of order 10 m, where the field ceases to be frozen-in. This is about four orders of magnitude below the current resolution limit of solar telescopes. The subpixel structuring has a dramatic effect on the derived, spatially averaged flux densities in the resolved domain, in particular on the angular distribution of the field. Thus we find that the previously reported apparent predominance of horizontal magnetic flux on the quiet Sun is an artefact of the subresolution structuring. Here we try to clarify how Stokes profile data may be used to explore the spatially unresolved domain.

## 1. Introduction

At resolved scales the magnetic Reynolds number is very large in the solar photosphere, but as we go down in scale it decreases until it becomes unity or less. This happens at a scale of about 10 m (de Wijn et al. 2009). Only at this small scale, which is four orders of magnitude smaller than the best spatial resolution of current solar telescopes, does the magnetic field cease to be frozen in to the plasma, so that the magnetic diffusion time scale becomes shorter than the convective time scale. Since the viscous diffusion limit for non-magnetic turbulence is much smaller still, we can expect the magnetic structuring produced by magneto-convection to continue all the way down to the 10 m scale. It follows that such structuring will not be resolved in any foreseeable future, and that therefore indirect methods to diagnose the magnetic structures in the spatially unresolved domain will always be indis-

pensible to properly understand the nature of solar magnetism and to interpret observational data.

Already in the 1960s it was recognized that such indirect diagnostic methods were urgently needed. Efforts in this direction led to the introduction of the two main tools to diagnose the magnetic fields in the spatially unresolved domain, the line-ratio technique with the longitudinal Zeeman effect (Stenflo 1973), and the Hanle effect (Stenflo 1982). While in stellar astronomy it has always been obvious that our knowledge must be based on indirect methods, the need has not been equally recognized among solar physicists. Each new advance in high-resolution imaging of solar magnetic fields has often conveyed the generally misleading impression that we are at the verge of resolving most of the fundamental magnetic structures.

---

*Send offprint requests to:* J. O. Stenflo

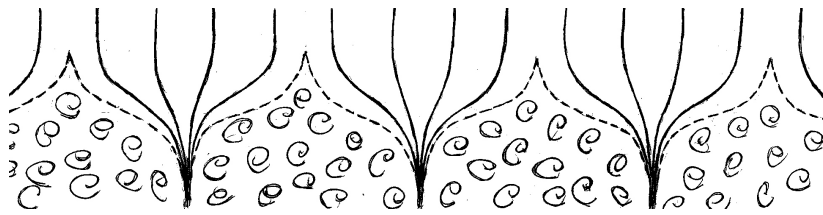


**Fig. 1.** In the standard model the subresolution quiet-Sun magnetism is composed of two main building blocks: flux tubes, which in the photosphere have field strengths of order 1 kG and a typical filling factor of 1 %, and the turbulent weaker field in between, which occupies the remaining 99 % of the volume. This dualistic view is much a consequence of using two complementary diagnostic tools, the Zeeman effect, which responds to the flux tubes but is blind to the turbulent field, and the Hanle effect, which responds in the opposite way.

## 2. Standard model

Empirical quantitative information on solar magnetic fields is obtained via spectropolarimetry. There are two types of effects that produce observable magnetic signatures in the Sun's spectrum: the Zeeman effect and the Hanle effect (cf. Stenflo 1994). The polarization signature relates to the magnetic field in a non-linear way that depends on the spectral line and the physical effect used. The line-ratio technique exploited the differential non-linear response of two spectral lines that were so chosen that the magnetic effects could be isolated from the thermodynamic effects. This led to the discovery that more than 90 % of the total photospheric flux was due to intrinsically strong (1-2 kG) fields with small magnetic filling factors, typically 1 % for the quiet Sun (Stenflo 1973). To reach such a conclusion a 2-component model had been introduced, based on the assumption that the atmosphere can be split in a "magnetic" component with a certain filling factor, and a "non-magnetic" component representing the remaining (typically 99 %) of the volume. The theoretical scenario was magnetic flux tubes embedded in a field-free environment. A whole industry of flux tube models at ever higher levels of sophistication emerged (cf. Solanki 1993).

Since it was obvious that the highly conducting solar plasma cannot harbor such field-free regions, and that the notion of a "non-magnetic" component was an idealization introduced merely for the sake of extracting the

properties of the magnetic component with the line-ratio approach, the next challenge became to find an appropriate diagnostic tool to extract the magnetic properties of the component that had been labeled as "field free". After magnetic line-broadening had been found to provide some constraints (Stenflo & Lindegren 1977), the Hanle effect was introduced and found to be the by far most useful tool for this domain of solar magnetism. This led to the discovery of a ubiquitous turbulent magnetic field of intermediate strength filling 99 % of the photospheric volume (Stenflo 1982; Trujillo Bueno et al. 2004).

These efforts led in the early 1980s to what we can now refer to as the "standard model" for quiet-Sun magnetism in the spatially unresolved domain, illustrated in Fig. 1. The dualistic nature of the model is however much a consequence of having two highly complementary diagnostic tools at our disposal, which give us two filtered versions of reality. When we "put on our Zeeman goggles" we project out a world of flux tubes, while when we put on our "Hanle goggles" we see the turbulent aspects of solar magnetism. In contrast, numerical simulations of magneto-convection indicates a continuous world best described in terms of probability density functions (PDFs). If we would describe the standard model of Fig. 1 in terms of PDFs it would appear rather odd: The PDF would be composed of two discrete,  $\delta$ -function like peaks, one near a field strength of 1 kG representing nearly vertical fields, the other peak at intermediate field strengths (around 30-60 G)

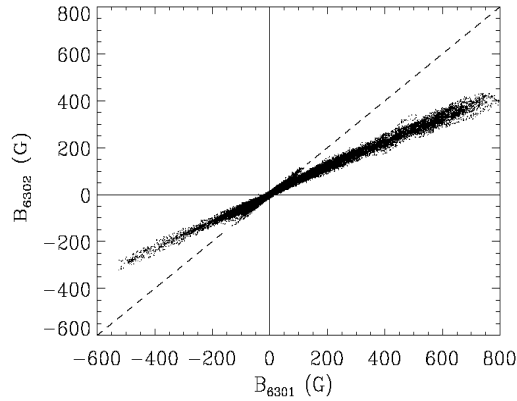


**Fig. 2.** If the magnetic fields in the Hinode data set were spatially resolved, the points in the scatter plot of the flux densities  $B_{6302}$  vs.  $B_{6301}$  would fall along the dashed line with a slope of unity. Instead the great majority of points fall along a line of slope between 0.6 and 0.7, which is consistent with intrinsic kG field strengths. However, for small flux densities we find a weaker population of points that nearly follows a slope of unity.

with a nearly isotropic angular distribution. As the filling factor for the strong fields is of order 1 %, the second peak for the isotropic fields has about 100 times larger amplitude than the strong-field peak for the vertical fields.

As this 2-peak representation of the PDF is much an artefact of our idealization with a 2-component model, which was tailor-made to suit the Zeeman and Hanle diagnostic tools, our next task should be to try to transcend the 2-component approach and fill the “desert” between the two peaks of the “standard-model PDF”. Note that the 2-component concept with a magnetic filling factor has long been a standard diagnostic tool also in explorations of stellar magnetic fields, so the diagnostic tools beyond the 2-component model that we would develop for the Sun would naturally relate to stellar physics as well. Let us however next illustrate direct evidence for ubiquitous subpixel structuring in the Hinode data.

### 3. Evidence for subpixel structuring in the Hinode data

From magnetograms that represent maps of the signed polarization amplitude in a chosen spectral line it is impossible to conclude whether the structures displayed by the map

are spatially resolved or not. Evidence for subpixel structuring has to come from other types of additional information, which is available in the Stokes vector spectra recorded by the SOT/SP instrument on the Hinode satellite. Here we illustrate some properties of Hinode recordings of the quiet Sun at disk center. Of particular importance in this context is that the Hinode spectral window contains two iron lines of the same multiplet, Fe I 6301.509 and 6302.502 Å, from which various kinds of line ratios can be formed. These two lines do not allow the thermodynamic and magnetic effects to be directly separated, since the two lines in contrast to the optimum line-ratio pair 5250.22/5247.07 have different line strengths and therefore are influenced differently by the thermodynamics. Still the line ratios that we can form reveal in a direct and unambiguous way the existence of magnetic structuring far beyond the Hinode resolution limit (of 0.3 arcsec).

One classical way of applying the line-ratio technique is to plot the apparent flux densities measured in the two lines,  $B_{6302}$  and  $B_{6301}$ , against each other. No theoretical modelling is used in getting these flux densities from the measured circular polarization, only the assumption that the field is spatially resolved,

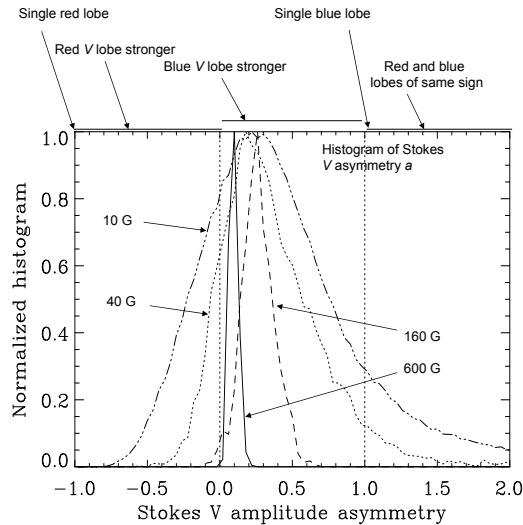


**Fig. 3.** The histograms for the Stokes  $V$  asymmetries are extremely broad for the weakest flux densities but become narrower as the flux density increases, while remaining systematically offset from zero asymmetry. These asymmetries are caused by subpixel correlations between the spatial gradients of the magnetic field and the velocity field, showing that the fields in the Hinode data set are far from spatially resolved (in particular for the weakest flux densities).

and that therefore the polarization is proportional to  $\partial I/\partial\lambda$ , the derivative of the simultaneously observed Stokes  $I$  (intensity) profile. If this assumption would be valid, then all the points should fall along the  $45^\circ$  (dashed) line of slope unity (see Fig. 2). Instead they fall along a well-defined regression line with a much smaller slope, between 0.6 and 0.7. We also notice a weaker population of points in the region of small flux densities (below about 100 G), which fall near the  $45^\circ$  line, although even for the smallest flux densities the dominant population is the one with the much smaller slope. The magnitude of the slope of the dominant population is in the framework of a 2-component interpretation consistent with field strengths of order 1 kG.

Line ratios need not only be formed from the Stokes  $V$  profiles, but complementary information is obtained from line ratios of Stokes  $I$ ,  $Q$ , or  $U$  profile parameters. They provide independent confirmation of magnetic structuring on subpixel scales. Such confirmation however also comes from the particular shapes of

the Stokes profiles. We will illustrate this here in terms of the Stokes  $V$  asymmetries.

The Stokes  $V$  amplitude asymmetry  $a$  is defined as

$$a = \frac{V_{\text{blue}} + V_{\text{red}}}{V_{\text{blue}} - V_{\text{red}}}, \quad (1)$$

where  $V_{\text{blue,red}}$  are the signed amplitudes of the blue or red wing lobes of the Stokes  $V$  profile. In a static atmosphere the Stokes  $V$  profiles are always anti-symmetric, which means that  $V_{\text{blue}} = -V_{\text{red}}$ , and therefore  $a = 0$ . Non-zero values of  $a$  are only possible if there is sub-resolution magnetic structuring with correlations between the gradients of the magnetic and the velocity fields (Stenflo et al. 1984; Steiner 2000; Sigwarth 2001). The larger the asymmetry is, the greater is the influence of this subpixel structuring.

Figure 3 shows a set of histograms of the Stokes  $V$  asymmetry for the disk-center quiet-Sun Hinode Stokes  $V$  profiles of the Fe I 6301 Å line. Each curve represents an asymmetry histogram for a narrow range of flux densities centered around the respective values

indicated in the figure. While being narrow but significantly offset from zero for large flux densities, the distributions get extremely broad as we go down to small flux densities. This large spread is not caused by noise but is really solar. It shows that all the pixels, and in particular those with very small flux densities, represent areas with very significant subpixel structuring, which leads to such dramatically distorted Stokes profiles.

#### 4. Influence of subpixel structuring on the determination of spatially averaged distribution functions

The statistical properties of the inhomogeneous magnetic field can be conveniently characterized by probability density functions (PDFs) for the vertical, horizontal, and total flux densities as well as by the angular distribution of field vectors (which in turn is a function of flux density). To confront theory with observations we need to compare these distribution functions as derived from numerical simulations with those derived from observations. While we cannot derive empirical distribution functions for the “intrinsic” field, since this would require infinite spatial resolution, an achievable objective may be to derive them for the flux densities that refer to quantities averaged over the angular resolution element of the instrument used. It might seem that it would be straightforward to do this from the observed longitudinal and transverse magnetograms, but this is far from the case.

To highlight this difficulty with a concrete example, let us recall that Lites et al. (2008) concluded from an analysis of Hinode SOT/SP quiet-Sun data at disk center that there is five times more horizontal than vertical magnetic flux in the photosphere. Subsequently Schüssler & Vögler (2008) reported that their numerical simulations of magneto-convection found the same dominance of horizontal flux, which was taken as evidence that the fields are generated by a local near-surface dynamo. I have however recently analysed the identical Hinode data set and come to the opposite conclusion, namely that it is the vertical flux that dominates.

The main reason for such a profound difference in the derived field structure is to be found in the way one accounts for the influence of the subpixel magnetic structuring on the process of averaging across the angular resolution element. The problem is that the relation between polarization and field strength is not linear, and that the non-linearities are much bigger and entirely different for the linear polarization as compared with the circular polarization. Because of these non-linearities the way in which the magnetic field is structured on subresolution scales has a dramatic influence on the meaning of the average over a pixel.

While these effects are modest for the circular polarization, they are huge for the linear polarization. This is why one can get major systematic errors in the field inclination, which is based on the combined use of the circular and linear polarizations. For instance, if one for a magnetic field with subpixel structuring bases the interpretation of the linear polarization on the incorrect assumption that the field elements are resolved (and thus homogeneous across the resolution element), then this may lead to an overestimate of the transverse flux density by a large factor.

Using the line-ratio information in the Hinode data to allow us to model and account for the effect of the subpixel structuring on the transverse and longitudinal flux densities, we find an angular distribution of the field vectors that is nearly isotropic for the smallest flux densities, but which quickly gets increasingly peaked around the vertical direction as the flux density increases. If we describe the angular distribution in terms of the power law  $\mu^\alpha$ , where  $\mu$  is the cosine of the angle of inclination with the vertical direction, then the exponent  $\alpha$  is found to be proportional to  $B^2$ , where  $B$  is the flux density.  $\alpha = 0$  represents the isotropic case, while larger  $\alpha$  values represent distributions that are more peaked around the vertical.

Earlier empirical PDFs in published literature for the horizontal and total flux densities appear to have their maxima distinctly offset from zero. At first sight this appears to be the case for the Hinode data set as well (cf. Lites et al. 2008), but more detailed analysis

reveals this to be an artefact of noise. When the noise effects are eliminated we find that all PDFs for the quiet Sun, not only for the vertical flux density but also for the horizontal and total flux densities, all have their maxima at zero flux density.

## 5. Outlook

Since we on the quiet Sun always deal with spatially unresolved magnetic structures, we should consistently avoid using the term “field strength” for observed fields but instead speak about flux densities. Only in the limit of infinite angular resolution do the two concepts become synonymous.

In the past several decades spatially unresolved magnetic fields have been diagnosed in terms of the 2-component interpretational model, also when Hanle effect observations have been included. Since however a 2-component model would have a PDF consisting of two discrete  $\delta$  function peaks, which is unphysical as there are strong reasons to expect the true PDFs to be smooth, continuous functions, there is a clear need to transcend the 2-component model towards more realistic interpretational models. Since we have no direct information about the shapes of the PDFs in the spatially unresolved domain, we need to explore the scaling laws of the PDFs in the resolved domain to find out to what extent they can be extrapolated into the unresolved domain. Such extrapolation would not be possible or meaningful if it were not for the high degree of scale invariance of the magnetic pattern that has been indicated by earlier studies (Stenflo & Holzreuter 2002, 2003). The scale invariance appears to be a consequence of the fractal-like nature of the magnetic pattern as we zoom in on ever smaller scales. Theoretical considerations and numerical simulations of magneto-convection (e.g. Janßen et al. 2003; Stein & Nordlund 2006) should help us understand the origin of this fractal-like behavior and its scaling laws. When theory will be able to reproduce the empirical distribution functions at resolved scales, then we can have more confidence that it can provide us with scaling laws that go well beyond the current spatial resolu-

tion limit, although the 10 m magnetic diffusion scale will be far beyond the reach of the simulations.

*Acknowledgements.* I am grateful to Bruce Lites for introducing me to the wonderful Hinode SOT/SP data set. Hinode is a Japanese mission developed and launched by ISAS/JAXA, with NAOJ as domestic partner and NASA and STFC (UK) as international partners. It is operated by these agencies in co-operation with ESA and NSC (Norway).

## References

- de Wijn, A. G., Stenflo, J. O., Solanki, S. K., & Tsuneta, S. 2009, *Space Science Reviews*, 144, 275
- Janßen, K., Vögler, A., & Kneer, F. 2003, *A&A*, 409, 1127
- Lites, B. W., Kubo, M., Socas-Navarro, H., et al. 2008, *ApJ*, 672, 1237
- Schüssler, M., & Vögler, A. 2008, *A&A*, 481, L5
- Sigwarth, M. 2001, *ApJ*, 563, 1031
- Solanki, S. K. 1993, *Space Science Reviews*, 63, 1
- Stein, R. F., & Nordlund, Å. 2006, *ApJ*, 642, 1246
- Steiner, O. 2000, *Sol. Phys.*, 196, 245
- Stenflo, J. O. 1973, *Sol. Phys.*, 32, 41
- Stenflo, J. O. 1982, *Sol. Phys.*, 80, 209
- Stenflo, J. O. 1994, *Solar Magnetic Fields — Polarized Radiation Diagnostics*. (Kluwer)
- Stenflo, J. O., & Holzreuter, R. 2002, in *SOLMAG 2002. Proceedings of the Magnetic Coupling of the Solar Atmosphere Euroconference*, ed. H. Sawaya-Lacoste, ESA Special Publication, 505, 101–104
- Stenflo, J. O., & Holzreuter, R. 2003, in *Current Theoretical Models and Future High Resolution Solar Observations: Preparing for ATST*, eds. A. A. Pevtsov & H. Uitenbroek, *Astronomical Society of the Pacific Conference Series*, 286, 169
- Stenflo, J. O., & Lindgren, L. 1977, *A&A*, 59, 367
- Stenflo, J. O., Solanki, S., Harvey, J. W., & Brault, J. W. 1984, *A&A*, 131, 333
- Trujillo Bueno, J., Shchukina, N., & Asensio Ramos, A. 2004, *Nature*, 430, 326